XII National and III International

Conference on Engineering Thermodynamics

12CNIT-2022 - FULL PAPER

Indoor Daylight Model for All-Sky-Type Luminance Patterns

Diego Granados López[1], Manuel García Fuente[1], David González Peña[1,2], Montserrat Diez Mediavilla[1,2], Cristina Alonso Tristán[1,2]

[1]Research Group Solar and Wind Feasibility Technologies, SWIFT. Electromechanical Engineering Department. Avda. Cantabria s/n. 09006. Burgos, Spain. dgranados@ubu.es

[2] UIC-022, Junta de Castilla y León. Electromechanical Eng. Dep. EPS. Universidad de Burgos. Avda. Cantabria s/n, 09006, Burgos, Spain.

Keywords: *luminance pattern; all-sky model; daylight; energy efficiency*

TOPIC: Energy efficiency and sustainability in buildings and industry

1. Introduction

Daylighting is a design concept of buildings recognized as a key strategy in reducing the energy consumption and improving visual comfort and well being of their occupants [1]. According to the International Energy Agency (IEA), artificial lighting makes up 14% of electrical consumption in the European Union and 19% worldwide [2]. In addition to improve the energy efficiency of buildings, it has been demonstrated that daylighting has positive effects on human health and productivity [3]. Energy standards strongly recommend incorporating daylighting strategies into building design. However, daylighting design is complex due to its changing nature. Likewise improving the occupants' life, daylight implementation is also related to technical and architectural solutions such as heating and cooling [4]. Therefore, it is necessary balancing the positive health effects and energy savings in artificial lighting with the the possible thermal and visual discomfort caused by excessive sunlight penetrations and glare [5].

Currently, metrics such as the Average Daylight Factor (ADF) [6,7], International Standards and regulations as the Illuminating Engineering Society of North America (IESNA) [8], the European Commission [9], and the ISO 52000-1 [10] or independent researchers [1][11], have already faced this problem.

Traditionally, the Average Daylight Factor (ADF) was established as a recognized criterion by the prestigious Building Research Establishment (BRE) [6], and supported by the scientific community [12,13]. Daylight factor is the ratio between indoor illuminance and outdoor illuminance, measured for a specific point or for an average of a space. By definition, daylight factor should be calculated only under the CIE overcast sky condition. Therefore, ADF allows a stable characterization of the luminous environment by eliminating the dependence of the temporal variable and the orientation of the study. However, the annual average number of sunny days in Europe varies enormously. For example, the annual average of sunny days in Hamburg, Germany is 50 while in Madrid, Spain it is 194 [14]. Consequently, in locations with a high frequency of sunny skies, ADF,can not be considered as adequate index for indoor daylight availability [15]. Other studies [1,16] have developed dynamic metrics, considering the variability of natural lighting. If the frequency distribution of indoor lighting is known, Annual Sunlight Exposure (ASE) [17] and Daylight Autonomy (sDA) [8] at the given work plane, can be calculated, representing specific aspects of daylight, as shown in Table 1.

Table 1. Annual dynamic metrics for daylighting evaluation considering occupied hours (08:00-18:00 h).

Metric	Temporal Analysis (in a point in a space)	Target
Annual Sunlight Exposure (ASE)	Frequency of occurrency at a point on the working plane that receives sunlight greater than a threshold value (1000 lux) [18].	Analysing the intensity of lighting levels that causes visual discomfort
Spatial Daylight Autonomy (sDA)	Frequency of occurrency at a point on the working plane where a minimum illuminance threshold of 300 lux can be maintained by daylight [18].	Summarizing the frequency in which an illuminance threshold can be maintained by natural light on its own.

This study proposes the use of the DeLight method [20] for modeling indoor illuminance taken into account all-sky conditions. As main novelty of this study, the sky conditions will be experimentally determined from luminance pattern of the sky. Nevertheless, this study has adapted it to the CIE Standard sky luminance distribution model [21].

2. DeLight method description

DeLight is a compact daylight simulation tool, developed at Helsinki University of Technology [20]. This tool is a Light Transfer Model that allows the calculation of indoor illuminance on the surfaces of interest, e.g. on the horizontal surface at a desk level. A simulation can be performed for a single point in time and exterior daylight availability, or on a timestep basis for a specified run period using either theoretical or measured weather data. Interior daylight levels can be calculated for a single reference point, or for multiple points throughout a space to analyze the spatial distribution of light. The simulation model DeLight needs the sky luminance pattern, directly measured by means of a sky-scanner device, modeled by a sky luminance model, like Perez all-weather sky model [22,23] or directly derived from the CIE standard sky [24], previous determination of the sky conditions.

When the sky luminance distribution is known, it is possible to calculate the interior diffuse daylight illuminance. The calculation of the interior beam illuminance is quite straightforward, given the position of the sun and the room geometry if the sky luminance distribution is known.

For each point p on the work plante, DeLight model selects a single patch of the sky from the luminance pattern, as Figure 1 shows. The indoor horizontal illuminance at the point p on the work plane of the room is calculated by Eq. 1. It splits the global illuminance into three components; diffuse, beam, and reflected indoor illuminance.

$$L_p = L_{p,D} + L_{p,B} + L_{p,R} \quad (1)$$

The beam component, $L_{p,B}$, is a function of the geometry of the room and the horizontal beam illuminance measured outdoors. A complete description of the calculation of the $L_{p,B}$, can be found in [20]. Diffuse, $L_{p,D}$, and reflected, $L_{p,R}$, components depend on the luminance patch, and the room geometry. Following the nomenclature shown in Fig. 2, they are calculated by Eq. 2 and 3, respectively:

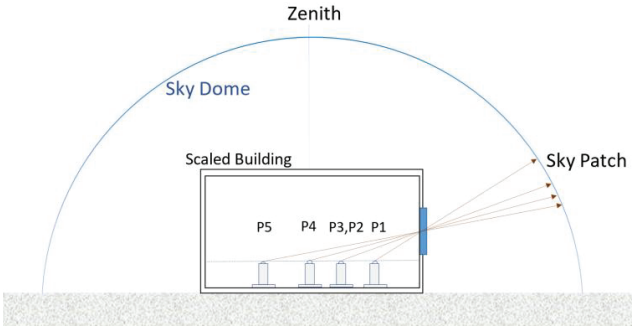

Figure 1. Ray traces from the sky Element.

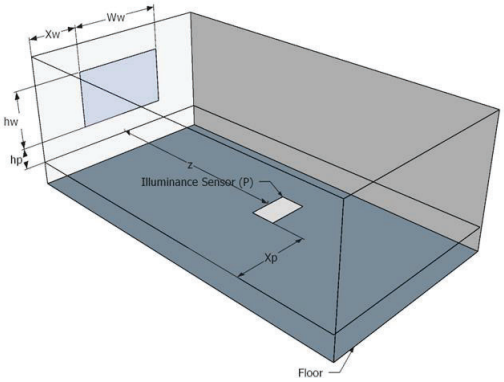

Figure 2. Nomenclature description for Eq. 2 and 3.

$$L_{p,D} = \frac{r_w L}{2}\left\{\frac{z}{\sqrt{h_p^2+z^2}}\left(\arctan\frac{x_w+w_w-x_p}{\sqrt{h_p^2+z^2}}+\arctan\frac{x_p-x_w}{\sqrt{h_p^2+z^2}}\right)+\right.$$
$$\left.\frac{z}{\sqrt{(h_p+h_w)^2+z^2}}\left(\arctan\frac{x_w+w_w-x_p}{\sqrt{(h_p+h_w)^2+z^2}}+\arctan\frac{x_p-x_w}{\sqrt{(h_p+h_w)^2+z^2}}\right)\right\} \quad (2),$$

$$L_{p,R} = \frac{r_w L\,\rho\,R_f}{2}\left[\left(\frac{h_w}{\sqrt{h_w^2+z^2}}\tan^{-1}\frac{w_w}{\sqrt{w_w^2+z^2}}+\frac{w_w}{\sqrt{w_w^2+z^2}}\tan^{-1}\frac{h_W}{\sqrt{w_w+z^2}}\right)+\right.$$
$$\left.2\left(\frac{w_w}{\sqrt{w_w^2+z^2}}\tan^{-1}\frac{h_w}{\sqrt{h_w^2+z^2}}+\frac{h_w}{\sqrt{h_w^2+z^2}}\tan^{-1}\frac{w_W}{\sqrt{h_w+z^2}}\right)\right] \quad (3).$$

z is the distance (m) between the window and the point p; L is the luminance of the patch that corresponds to the point p (lux); h_p is the height (m) between the bottom edge of the window and the point p (m); h_w is the height of the window (m); w_w is the width (m) of the window; $x_w$is the distance (m) between the left edge of the window and the left wall; and $x_p$is the distance between the reference point p and the left wall, as Figure 2 shows. ρ is the outdoor albedo, r_w is the visible light transmittance, and R_f is average indoor surface reflectance

The original design of Vartiainen [20] suggests considering only back reflections. But its model was modified by [21] to consider the influence of all interior walls as well.

3. CIE standar sky classification

The International Commission Illumination (CIE) [24] classification of skies establishes that the illuminance pattern of the sky can be modeled theoretically based on the position of the sun, location, and the type of sky. In this way, each sky type has associated coefficients that adjust the illuminance pattern to the theoretical formula decribed in equation 4.

$$L_a = \left(1 + c \cdot \left[e^{d\chi} - e^{\frac{d\pi}{2}}\right] + e \cdot \cos^2 \chi\right)\left(1 + a \cdot e^{\frac{b}{\cos Z_p}}\right) \quad (4)$$

Coefficients a, b, c, d, and e, Table 3, are defined by CIE [24] as functions of the sky type. Z_p is the zenith angle of the sky element and χ is the dispersizon angle, calculated from Equation (5):

$$\chi = arcos(\cos Z_s \cos Z_p + \sin Z_s \sin Z_p \cos|\Phi_p - \Phi_s|) \quad (5),$$

where Φ_p is the azimuth angle of the sky element, p, Z_s and Φ_s are the zenith and azimuth angles of the sun. The χ represents the shortest angular length between the sky element, p, and the sun, as it is shown in Figure 3.

Table 3. Parameters of CIE standard sky types [22].

Sky	a	b	c	d	e	Sky Description
I	4	−0.7	0	-1	0	CIE Standard Overcast Sky
II	4	−0.7	1	−1.5	0.5	Overcast, with steep luminance gradation and slight brightening towards the sun
III	1.1	−0.8	0	−1	0	Overcast, moderately graded with azimuthal uniformity
IV	1.1	−0.8	2	−1.5	0.15	Overcast, moderately graded, and slight brightening towards the sun
V	0	−1	0	−1	0	Sky of uniform luminance
VI	0	−1	2	−1.5	0.15	Partly cloudy sky, no gradation towards the zenith, slight brightening towards the sun
VII	0	−1	5	−2.5	0.3	Partly cloudy sky, no gradation towards the zenith, brighter circumsolar region
VIII	0	−1	10	−3	0.45	Partly cloudy sky, no gradation towards the zenith, the distinct solar corona
IX	−1	0.55	2	−1.5	0.15	Partly cloudy, with the obscured sun
X	−1	0.55	5	−2.5	0.3	Partly cloudy, with the brighter circumsolar region
XI	−1	0.55	10	−3	0.45	White-blue sky with the distinct solar corona
XII	−1	0.32	10	−3	0.45	CIE Standard Clear Sky with low polluted atmosphere

Sky	a	b	c	d	e	Sky Description
XIII	−1	0.32	16	−3	0.3	CIE Standard Clear Sky, polluted atmosphere
XIV	−1	0.15	16	−3	0.3	Cloudless turbid sky with the broad solar corona
XV	−1	0.15	24	−2.8	0.15	White-blue turbid sky with the broad solar corona

Trengeza proposed in 2004 [25] a modification of the original criterion to define the CIE sky type [26] for low latitude locations. The case of Burgos, where the most frequent CIE typologies in Burgos -overcast, partial, and clear- are the one, eight, and twelve, which corresponds to overcast with a steep gradation and azimuthal uniformity, partly cloudy, with a bright circumsolar region, and very clear/unturbid with a clear solar corona respectively [27]. Fig 3 shows a picture of the sky, the experimental luminance pattern, and the one predicted by the CIE standard.

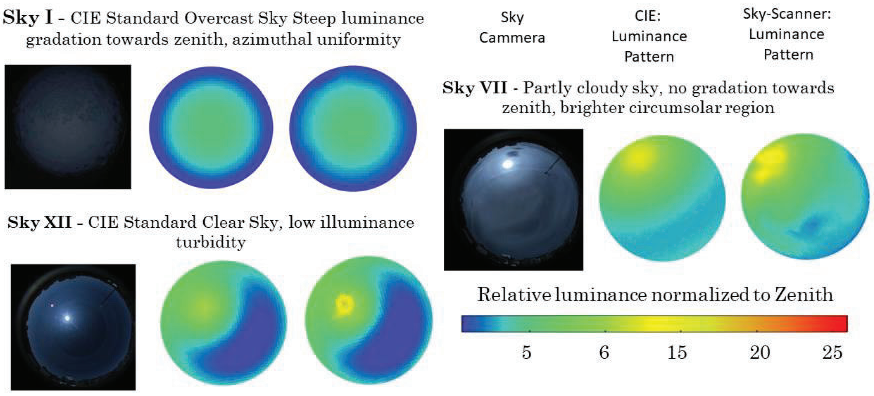

Figure 3. Example of luminance patterns. CIE sky type XII (recorded 2019/07/19 11:00 utc) ; CIE sky type I (recorded 2018/01/06 10:30 UTC). CIE sky type VII (recorded 2019/04/15 08:30 utc).

1. Case Study

This work proposes the use of the DeLight model [20] to predict indoor illuminance for all sky conditions. This work can improve the daylight integration during the building design stage. The inputs of the model are room geometry, sky luminance distribution, and diffuse illuminance.

A scale building, shown in Figure 4, and described in Table 3, has been set up for outdoor tests, in which indoor illuminance, sky luminance distribution, and diffuse illuminance data are registered every ten minutes during a experimental campaign extended from (from 01 July 2021 to 21 Aug 2021). Five luxmeters (model EKO ML 020P) were located inside the scaled room in the points described in Table 4, for recording the indoor illuminance.

Global and diffuse horizontal illuminance and beam illuminance are recorded in the meteological and radiative facility of the research group SWIFT, at University of Burgos, and described in previous works.The scale building is located in the same place that the meteorological station. The sky luminance distribution is determined using a Sky-scanner model EKO MS-321LR (SS), and the CIE standard sky classification (CIE).

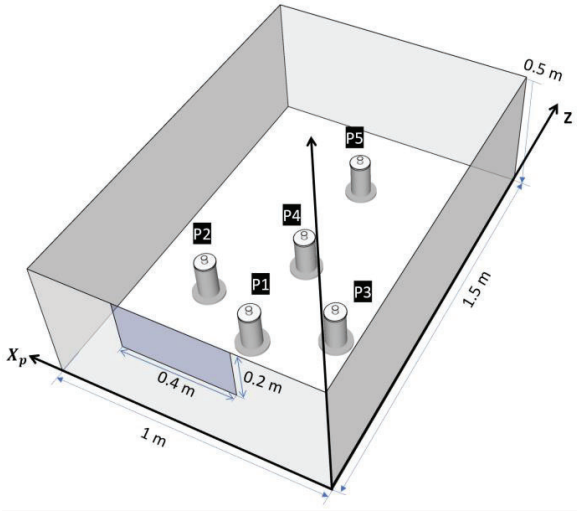

Figure 4. Model of the scale building prototype and location of the lux sensor.

Table 3. Properties and design of the scaled building.

Element	Properties		Ref.
Black indoor surfaces	Reflectance (R_f)	0.079	Reflectance and transmitance were tunned according to ASHRAE Guideline (2014) [28] at the facility.
3mm think glass	Transmittance (r_w)	0.74	
Ground surface (concrete and pavement)	Albedo (ρ)	0.5	[29]

Table 4. Location of the luxmeters inside the scaled building shown in Figure 3.

Parameters	P1	P2	P3	P4	P5
Z	0.375 m	0.5 m	0.5 m	0.75 m	1.1250 m
x_p	0.5 m	0.25 m	0.75 m	0.5 m	0.5 m

2. Results and discussion

The DeLight algorithm aims to model the buildings indoor illuminance components to obtain the illuminance distribution profiles in buildings. A great diversity of methods can be used for this purpose, implemented in different softwares like Daysim [30], Radiance [31], OpenStudio [32], HoneyBee [33], DIVA [34] or DesignBuilder [18]. To analyze DeLight goodness, experimental indoor illuminance measurements from the five luxometer have been recorded for all-sky conditions and compared with the DeLight model calculations at the same points. Two different values of the modeled illuminance at each point has been calculated: one using the experimental sky luminance pattern (SS), and other derived from the CIE standard sky previous caracterization of the sky type (CIE). The traditional statistical indicators Mean Bias Error, MBE (%), and Root Mean Square Error, RMSE(%), defined by Equations 6 and 7, have been used as goodness indices.

$$MBE = \frac{100\ \sum(X_{exp} - X_{mod})}{(N-1)\ \overline{X_{exp}}} \quad \text{(Eq. 6)},$$

$$RMSE = \frac{100}{\overline{X_{exp}}} \sqrt{\frac{\sum\left(X_{exp} - X_{mod}\right)^2}{N-1}} \quad \text{(Eq. 7)},$$

where X_{exp} is the experimental illuminance recorded at point p (1,2,3,4, and 5) by the luxmeters inside the scale building prototype, and X_{mod} is the DeLight modelled illuminance at the same point.

Table 5 shows the results of the statistical indices MBE and RSME calculated for each of the experimental points and for each of the sky luminance pattern. DeLight gets good performance in all locations when the experimental sky luminance pattern is used for calculations. In addition, the luminance pattern of the CIE standard proved to be very effective. Comparable results are found over the world [21,35].

Table 5. RMSE and MBE of each point of measure (P1, P2, P3, P4, and P5)

Location	DELIGHT MODEL	RMSE (%)	MBE
P1	SS	23.28	3.59
	CIE	18.89	-4.66
P2	SS	18.03	0.65
	CIE	18.45	-7.15
P3	SS	19.97	4.65
	CIE	16.07	-2.27
P4	SS	24.61	-4.77
	CIE	20.38	-4.60
P5	SS	24.26	6.85
	CIE	22.94	7.58

The IESNA [8] recommends a minimum level of 300 lux for an adequate development of the daily human activities. Therefore, illuminance levels higher than 1000 lux can cause glare and visual discomfort. Figure 5 shows the Frequency Of Occurrence (FOC, %) of a illuminance level higher than 300 lux (a) and 1000 lux (b), respectively, in the measurement points. The inner circle refers to experimental data, the middle one to DeLight predictions from SS, and finally, the outer one to DeLight predictions from CIE. According to this metrics.

The daylight illuminance widely varies across the work plane, from the front area, near the fenestration, to the backside of the room. Figure 5-a is the FOC of the luminance greater than 300 lux, that links with the recommended illuminance levels for humans [8]. According to this metric, the best locations are near the windows. Figure 5-b is the FOC of the luminance greater than 1000 lux, that links to the discomfort on humans [8]. It shows the strong dependence of the average illuminance with the size and position of the windows.

On the other hand, Figure 5 shows the high agreement of the predictions of DeLight model using the experimental luminance pattern and the DeLight model using the the CIE standard compared the experimental indoor measurements.

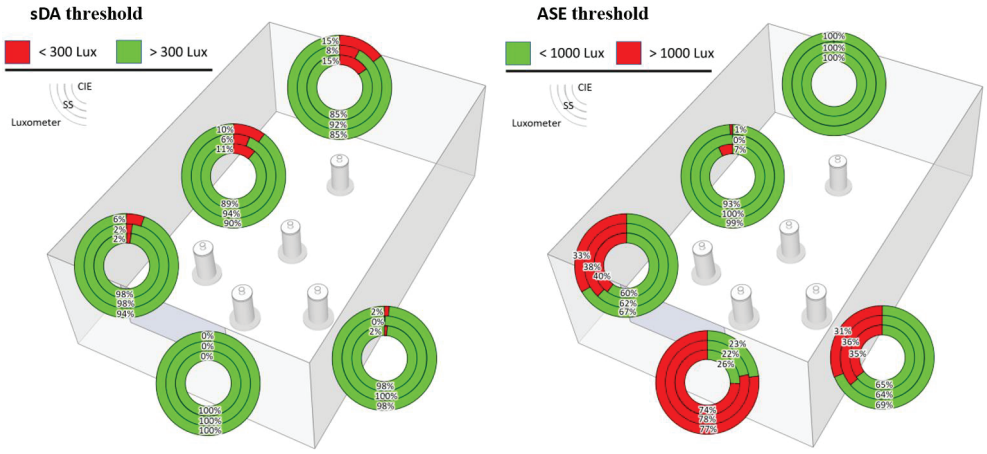

(a) (b)

Fig. 5. FOC of the sDA threshold (a), and ASE threshold (b). The inner circle refers to experimental data from luxometers, the middle one to DeLight predictions from SS, and finally, the outer one to DeLight predictions from CIE.

3. Conclusions

Daylight plays a fundamental role in human behavior and health and improve the energy efficiency in buildings. Main difficult to obtain the indoor illuminace distribution is the calculation of the contribution of the diffuse outdoor illuminance and the reflected component in each of the interior surfaces. DeLight uses a Light Transfer Model that simplifies the calculation of indoor illuminance, when the luminance pattern of the sky is known. This study case has compared the use of the luminance pattern directly derived from the CIE standard sky classification and the experimental luminace pattern determined by a sky scanner. Results has demonstrated that the CIE standard obtain good prediction of the indoor illuminance distribution.

The analysis distribution of the indoor illuminance allows stablished the visual comfort conditions in the building. When the study is done considering the occupied hours the needs of artificial lighting or shading devices can be determined. Therefore daylighting consideration at the design stage can contribute to energy efficiency and visual comfort in buildings.

Acknowledgments

Financial support provided by the Spanish Ministry of Science & Innovation (Ref. RTI2018-098900-B-I00) and PIRTU Program, ORDEN EDU/556/2019, for financial support.

References

[1] P. Tregenza, J. Mardaljevic, (2018) Daylighting buildings: Standards and the needs of the designer. *Lighting Research and Technology*. 50, 63–79.
[2] IEA, International Energy Agency. *Official Web-site*. ⟨http://Www.Iea.Org/⟩.
[3] P. MacNaughton, M. Woo, B. Tinianov, M. Boubekri, U. Satish, (2021) Economic implications of access to daylight and views in office buildings from improved productivity. *Journal of Applied Social Psychology*. 51, 1176–1183.
[4] G.S.O. Vathanam, K. Kalyanasundaram, R.M. Elavarasan, S. Hussain, U. Subramaniam, R. Pugazhendhi, M. Ramesh, R.M. Gopalakrishnan, (2021) A review on effective use of daylight

harvesting using intelligent lighting control systems for sustainable office buildings in India. *Sustainability*. 13.
[5] E.J. Gago, T. Muneer, M. Knez, H. Köster, (2015) Natural light controls and guides in buildings. Energy saving for electrical lighting, reduction of cooling load. *Renewable and Sustainable Energy Reviews*. 41, 1–13.
[6] B.R.E. (2011) Site Layout planning for daylight and sunlight.
[7] Cibse, (1999) Daylighting and window design. CIBSE, *Publicaciones IDAE*. LG10_1999, 8–98.
[8] M. Andersen, J. Ashmore, L. Beltran, J. Bos, D. Brentrup, K. Cheney, N. Digert, D. Eijadi, L.Fernandes, D. Glase, (2012) Approved Method: IES Spatial Daylight Autonomy (sDA) and Annual Sunlight Exposure (ASE), *Illuminating Engineering Society of North America, IES LM-83-12*.
[9] European Commission, (2020) In focus: Energy efficiency in buildings. *European Commission. – Department: Energy*.
[10] International Organization for Standardization (ISO), (2017) ISO 52000-1:2017 - Energy performance of buildings — Overarching EPB assessment — Part 1: General framework and procedures. *International standard*.
[11] E. Brembilla, C.J. Hopfe, J. Mardaljevic, A. Mylona, E. Mantesi, (2019) Balancing daylight and overheating in low-energy design using CIBSE improved weather files. *Building Services Engineering Research and Technology*. 0(0), 1–15.
[12] S.P.G. Bonaiuti, M. Wilson, (2007) An analysis of the (BRE) average daylight factor and limiting depth guidelines as design criteria. *2nd PALENC. Conference and 28th AIVC Conference on Building Low Energy Cooling and Advanced Ventilation Technologies in the 21st Century, September, Crete island, Greece*. 2, 739–745.
[13] A. Olina, N. Zaimi, (2008) Daylight prediction based on the VSC - DF relation. *Energy and Building Design Department of Architecture and Built Environment, Lund University*. Thesis: EEBD - xx/18. .
[14] J. Mardaljevic, J. Christoffersen, P. Raynham, (2013) A proposal for a European standard for daylight in buildings. *Lux Europa 2013 12th European Lighting Conference. Krakow, Polad*.
[15] J.Y. Suk, K. Kensek, (2011) Daylight Factor (overcast sky) versus Daylight Availability (clear sky) in Computer-based Daylighting Simulations. Comput. Daylighting Simulations.
[16] S. Darula, J. Christoffersen, M. Malikova, (2015) Sunlight and insolation of building interiors. Energy Procedia. 78, 1245–1250.
[17] J. Kaempf, B. Paule, (2016) Energy audit and inspection procedures. A Technical Report of IEA SHC Task 50. *Solar Heating and Cooling Programme. International Energy Agency*.
[18] DesignBuilder, (2021) helpv7.0.
[19] A.M. AL-Dossary, D.D. Kim, (2020) A study of design variables in daylight and energy performance in residential buildings under hot climates. *Energies*. 13,5836.
[20] E. Vartiainen, (2000) Daylight modelling with the simulation tool DeLight, Report TKK, *Helsinki University of Technology Publications in Engineering Physics*.
[21] C.-H. Kim, K.-S. Kim, (2019) Development of Sky Luminance and Daylight Illuminance Prediction Methods for Lighting Energy Saving in Office Buildings. *Energies*. 12,592.
[22] R. Perez, R. Seals, J.J. Michalsky, (1993) All-weather model for sky luminance distribution—Preliminary configuration and validation. *Solar Energy*. 50, 235–245.
[23] J.M. R Perez, R Seals, (1993) Erratum to all-weather model for sky luminance distribution — preliminary configuration and validation. *Solar Energy*. 51, 423.
[24] ISO 15469:2004(E)/CIE S 011/E:2003, (2004) Spatial distribution of daylight-CIE standard general sky. *ISO*.
[25] P.R. Tregenza, (2004) Analysing sky luminance scans to obtain frequency distributions of CIE Standard General Skies. *Lighting Research and Technology*. 36 (4), 271-281.

[26] R. Kittler, R. Perez, S. Darula, (1997) A new generation of sky standards, in: Lux Eur. *Proceedings of the Lux Europa Conference*. Amsterdam.1,359–373.
[27] A. Suárez-García, D. Granados-López, D. González-Peña, M. Díez-Mediavilla, C. Alonso-Tristán, (2018) Seasonal caracterization of CIE standard sky types above Burgos, northwestern Spain. *Solar Energy.* 169, 24–33.
[28] ASHRAE, (2021) ASHRAE Handbook-fundamentals. *ASHRAE Research*.
[29] P.A. Mirzaei, D. Olsthoorn, M. Torjan, F. Haghighat, (2015) Urban neighborhood characteristics influence on a building indoor environment. *Sustainable Cities and Society*. 19, 403–413.
[30] DAYSIM, (2021) *Official Web-site*.
[31] Radiance, (2021) *Official Web-site*.
[32] OpenStudio, (2021) *Official Web-site*.
[33] HoneyBee, (2021) *Official Web-site*.
[34] Solemma, (2021) Diva. *Official Web-site*.
[35] S. Yun, K.-S. Kim, (2018) Sky Luminance Measurements Using CCD Camera and Comparisons with Calculation Models for Predicting Indoor Illuminance. *Sustainability*. 10, 1556.